SF2A 2017
C. Reylé, P. Di Matteo, F. Herpin, É. Lagadec, A. Lançon, Z. Meliani, F. Royer (eds)

THE PHOTOSPHERE OF RED SUPERGIANT STARS AS SEEN BY OPTICAL INTERFEROMETRY

M. Montargès[1], P. Kervella[2], G. Perrin[2], A. Chiavassa[3], R. Norris[4], S. T. Ridgway[5] and L. Decin[1]

Abstract. During the end of their lives, massive stars become red supergiant (RSG) stars. At this stage, they are forging heavy elements in their cores that are transported up to the photosphere thanks to convection and expelled to the interstellar medium through the star's mass loss. Cooling in the outer atmosphere causes these elements to become molecules and dust that are the building blocks of future planetary systems and eventually life. One of the scenarios to explain the launch of material from the photosphere involves convection that leads to an increased scale height and facilitates mass ejection. We present here observations of several bright features on the surface of nearby RSG stars using near infrared (NIR) interferometry. They are interpreted as being the top of convective cells. We compare them with 3D convective simulation predictions. These inhomogeneities are bright and large enough to cause a photocenter displacement that might bias parallax measurements.

Keywords: stars: imaging - supergiants - stars: mass-loss - infrared: stars - techniques: interferometric

1 Introduction

The chemical enrichment of the Universe is driven by evolved stars. Red supergiant (RSG) stars represent one of the last evolutionary stages of massive stars. They experience an important mass loss (10^{-6} $M_{\odot}.yr^{-1}$ for Betelgeuse, Mauron & Josselin 2011). However, the mechanism driving this outflow has yet to be identified. A possible scenario involves convection lowering the effective gravity on the photosphere and allowing radiative pressure on molecular lines to launch the material (Josselin & Plez 2007).

The convective pattern of RSG stars has been observed for several years. Haubois et al. (2009) reconstructed the first high dynamic range image of Betelgeuse using IOTA H band observations. They observed two bright spots whose size was of the same order of magnitude as the stellar radius. These features were consistent with predictions from 3D radiative hydrodynamics (RHD) simulations (Chiavassa et al. 2010). Several inhomogeneities were observed on the photosphere of nearby RSG stars using near infrared (NIR) interferometry. With the high spectral resolution mode of VLTI/AMBER, upward and downward motions were observed in the CO shell surrounding Antares (Ohnaka et al. 2013, 2017) and Betelgeuse (Ohnaka et al. 2011). On the latter, Montargès et al. (2014) showed that their VLTI/AMBER observations were compatible with the presence of convective features on the K band photosphere.

To better understand the role of the convective cells in initiating the mass loss of RSG stars, times series need to be acquired, in order to determine the evolution timescale of the convective features and to obtain a statistics of their morphological characteristics. These elements can be used to challenge the quality of the numerical models that are unable, for now, to reproduce the molecular extension of the atmosphere of RSGs nor their terminal wind velocity. We present here observations* of the nearby RSG stars Betelgeuse and Antares that are interpreted using analytic models (Sect. 2) and preliminary reconstructed images of CE Tau, a RSG located farther away (Sect. 3).

[1] Institute of Astronomy, KU Leuven, Celestijnenlaan 200D B2401, 3001 Leuven, Belgium
[2] LESIA, Observatoire de Paris, PSL Research University, CNRS, Sorbonne Universités, UPMC Univ. Paris 06, Univ. Paris Diderot, Sorbonne Paris Cité, 5 place Jules Janssen, 92195 Meudon Cedex, France
[3] Université Côte d'Azur, Observatoire de la Côte d'Azur, CNRS, Lagrange, France
[4] Center for High Angular Resolution Astronomy, Georgia State University
[5] National Optical Astronomy Observatories, 950 North Cherry Avenue, Tucson, AZ 85719, USA

*Obtained with ESO telescopes at Paranal Observatory, under ESO programs 288.D-5035(A), 090.D-0548(A), 092.D-0366(A, B), 094.D-0869 (A), 093.D-0378(A, B, C), 093.D-0673(C), and 298.D-5005(A, B)

2 Analytic models on Betelgeuse and Antares

2.1 Giant convective cells on Betelgeuse

Betelgeuse (α Ori) was observed on the nights of 2012 January 31, 2013 February 09, 2014 January 11, and 2014 November 21 using ESO's Very Large Telescope Interferometer (VLTI) instrument PIONIER (Precision Integrated-Optics Near-infrared Imaging ExpeRiment, Le Bouquin et al. 2011). Squared visibilities and closure phases were obtained on the compact configuration (stations A1-B2-C1-D0) of the Auxiliary Telescopes (AT), on baselines ranging from 11.3 to 35.8 m on the ground. PIONIER sample the H band with a spectral resolution of 40. On the four epochs, the first lobe of the squared visibilities presents an unusual dependency on the position angle (PA, Fig. 1, left). This means that the fitted angular diameter for a uniform disk (UD) or a limb-darkened disk (LDD) depends on the azimuth: the difference reaches 10% for the 2013 epoch. Therefore, a classical disk model cannot reproduce these data. Presenting strong deviations from 0° and 180°, the closure phases indicate the presence of asymmetries (Fig. 1, right). This excludes an elliptical model.

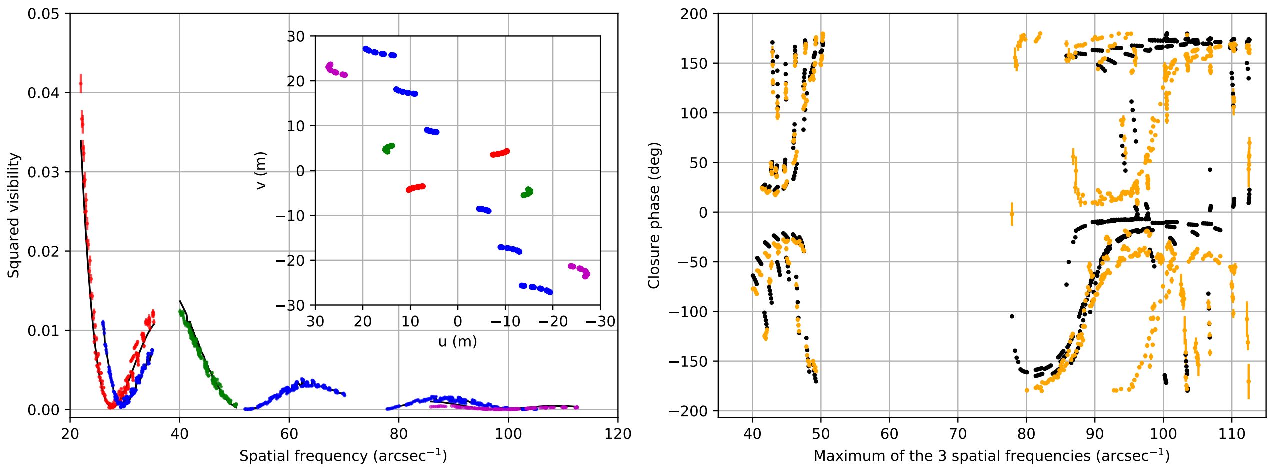

Fig. 1. Fit of the PIONIER data of Betelgeuse of February 2013 by the LDD and gaussian hotspot model. Only spatial frequencies lower than 51 arcsec^{-1} were considered. *Inset in the left image:* PA color-coded (u, v) coverage. *Left:* squared visibilities with matching colors. The black continuous line corresponds to the best fit model. *Right:* closure phases. The best fit model is represented in black.

Owing to previous observations of bright large spots on the surface of RSG stars, we fitted our observations with a power-law limb-darkened disk (Hestroffer 1997) on which we added a bright gaussian spot. The complete description of the model and of the fitting process is detailed in Montargès et al. (2016). As shown for the 2013 epoch on Fig. 1, this model fits both the squared visibilities and the closure phases. In particular, it is able to reproduce the doubling of the first lobe as a function of the PA. In this model, the resulting angular diameter of the star is correlated to the characteristics of the bright spot. This means that the presence of such structure can bias the angular diameter estimation of a star if its first lobe is probed on a single PA direction.

A bright spot can be fitted in all datasets except for the last epoch. In this case, it is necessary to introduce a second feature, dimmer and smaller. Figure 2 represents the corresponding intensity maps for the four epochs. The photocenter displacement we derived from these maps can reach up to 2 mas, more that a third of the parallax of the star (Harper et al. 2017). The position of this bright feature is consistent with spectropolarimetric measurements obtained at the Telescope Bernard Lyot with the Narval instrument (Aurière et al. 2016).

We compared our VLTI/PIONIER observations with 3D RHD simulations. Contrary to previous interferometric data (Chiavassa et al. 2010; Montargès et al. 2014), our squared visibilities and closure phases were not reproduced by the numerical models. 3D RHD simulations are unable to produce spots large and bright enough. Therefore, we proposed that Betelgeuse entered a convective regime dominated in the visible hemisphere by a large convective cell. This structure modifies the global convective pattern which can explain why the higher spatial frequencies (longer baselines, smaller convective structure on the photosphere) cannot be reproduced by the simulations either.

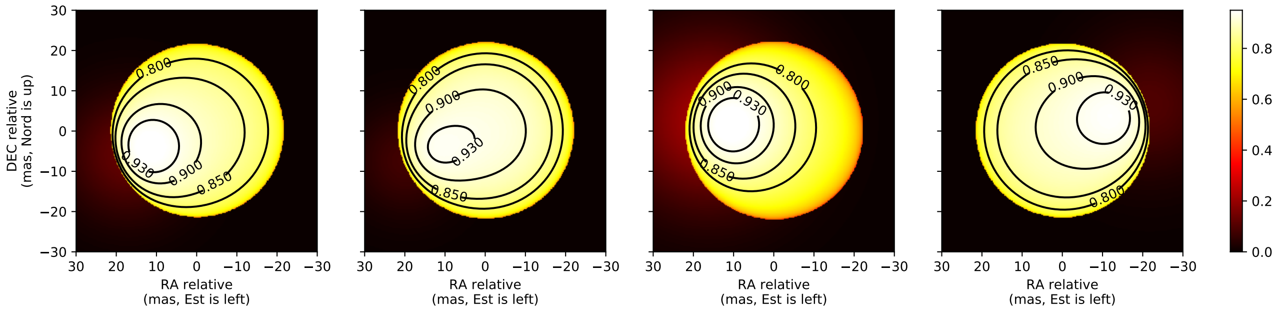

Fig. 2. Intensity maps associated to the best fit LDD and gaussian bright spot model on the PIONIER data of Betelgeuse. *From left to right:* January 2012, February 2013, January 2014, and November 2014.

2.2 *Characterizing the convective pattern of Antares*

We observed Antares with VLTI/PIONIER in its high spectral resolution mode on 2014 April 24, 29 and May 4 and 7 using the three available configuration of the AT. The spatial frequencies below 50 arcsec^{-1} cannot be reproduced by a regular disk model. However, deriving the angular diameter as a function of the PA allows to obtain a reliable estimation for each angle probed by the data. This results in an average LDD diameter of 38.27$\pm$0.37 mas at 1.61μm. Our observations probe the visibility function up to the sixteenth lobe of the visibility function. This corresponds to an angular resolution of 6% of the angular diameter. Chiavassa et al. (2011) showed that the convective pattern of RSG stars should host cells of various sizes, including small structures that should be the most numerous. Therefore, we cannot fit a single large structure on the photosphere as we did on Betelgeuse (Sect. 2.1). We adapted this previous model to derive the squared visibility and the closure phase associated to a LDD with distributions of bright spots of a fixed size. The detailed definition and expression of this model are given in Montargès et al. (2017). The deviations from the LDD model are best reproduced when using spot distributions with characteristic sizes of 17 and 2 mas, meaning 45% and 5% of the star angular diameter. With this model, the best fit angular diameter is 37.89 ± 0.10 mas at 1.61 μm. As concluded from the analysis of the VLTI/PIONIER datasets of Betelgeuse, the presence of photospheric features on a RSG star has direct consequences on the measurement of the angular diameter by optical interferometry.

This result directly affects the fit by the 3D RHD simulations. Indeed, the convective models are scaled to the angular diameter of the star. However, we demonstrated that the presence of features biases the fit of UD and LDD models. For this dataset on Antares, we set the angular diameter as a free parameter of the simulation. Figure 3 represents the best χ^2 on all the rotation angles and temporal snapshots of the simulation st35gm03n13 (Chiavassa et al. 2011) for a sample of angular diameters. The minimum χ^2 is reached for an angular diameter smaller than the value derived for a single LDD model and even a LDD with spot distributions model. The angular diameter measurement derived from NIR interferometry is strongly sensitive to the presence of features on the stellar surface, but also to their morphology. The best match was obtained for the LDD and spot distributions model. This indicates that features are present on the photosphere of Antares but that the current available 3D RHD simulations do not reproduce them correctly. This is in contradiction with previous results obtained on Betelgeuse (see references in Sect 2.1) but we stress that this Antares dataset probes previously unexplored region of the visibility function.

3 Image reconstruction on CE Tau

In September 2016, a spectropolarimetric signal was observed with the TBL/Narval instrument on CE Tau (Tessore et al. in prep.). It was the same signature as the previous observation of Betelgeuse (Sect. 2.1). This indicated the presence of photospheric features. With its ~ 10 mas angular diameter, CE Tau emerges as an interesting target for optical interferometry. Indeed, the two inner AT configurations allow to get a good sampling of the first three lobes of the visibility function, thus permitting an image reconstruction. In order to compare the feature detection with Narval with a NIR image, we observed this RSG star on 2016 November 14 and 22, and December 23 with VLTI/PIONIER. We used the high spectral resolution mode of the instrument. These observations will represent a joint diagnosis of the convective cell presence on the photosphere of CE Tau. On November 14, we used the AT in the compact configuration (A1-B2-C1-D0). On a star with the angular

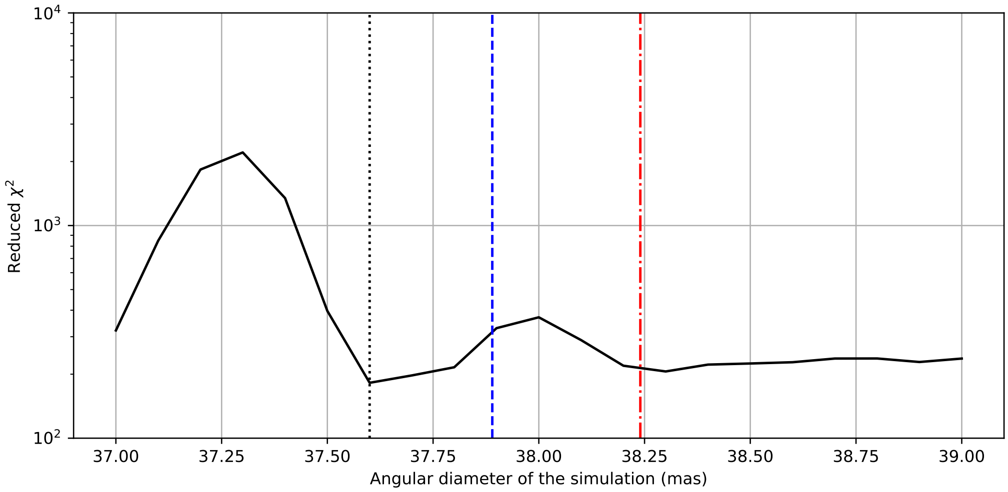

Fig. 3. Comparison of the VLTI/PIONIER squared visibilities of Antares at 1.61 μm with the 3D RHD simulation st35gm03n13. The black continuous line corresponds to the minimum χ^2 obtained over all the rotation angles and temporal snapshots of the simulation as a function of its angular diameter. The vertical black dotted line corresponds to the angular diameter giving the minimum χ^2. The red vertical dashed-dotted line corresponds to the angular diameter of the best fitted LDD model. The blue dashed line corresponds to the angular diameter of the best fitted LDD with spot distributions model.

diameter of CE Tau, these baselines probe only the first lobe of the visibility function. On November 22 and December 23, the AT were in the intermediate configuration (stations D0-G2-J3-K0). These data reach the second and third lobes: this means that features on the star are resolved. We decided to consider the November 14 data as "short spacing" observations, in an analogy with radio interferometry. With these baseline lengths, the star is not resolved and we can consider its general shape as invariant over a duration of a month. This assumption is confirmed by the intermediate configuration data: while data of the second and third lobe change between November and December, the part of the first lobe that is probed by these observations remain the same. The November 14 data were merged with the November 22 data to create a November dataset on the one hand, and with the December 23 observations on the other hand (December dataset).

For these two datasets, we reconstructed images using `SQUEEZE`, a compressed sensing based image reconstruction tool (Baron et al. 2010). `SQUEEZE` produces a mean reconstructed image that is the result of an exploration of the probability space using Monte Carlo Markov Chains. The detail of the reconstruction process as well as the images are presented in a forthcoming paper (Montargès et al. subm.).

4 Conclusions

We presented NIR interferometry observation of three nearby RSG stars. Several techniques were used to analyze these datasets: fit with classical disk models and with disk models including photospheric structures, comparisons with 3D RHD convective simulations and image reconstructions. Photospheric inhomogeneities are detected on the three stars. For Betelgeuse, we were able to follow the evolution of these structures over different epochs. The photosphere of RSG stars host a convective regime dominated by giant cells whose size reaches a significant fraction of the stellar radius. A smaller granulation is also detected on the high angular resolution data of Antares.

In the case of Antares and Betelgeuse, convective numerical simulations do not reproduce the convective pattern. These models are missing one or several ingredients: this can be for example the rotation or the magnetic field. The characterization of convection is crucial to understand its consequences on the mass loss of RSG stars but we have also shown that the presence of convective features can bias our angular diameter measurements using NIR interferometry and the parallax estimations.

We are grateful to ESOs Director-General, Prof. Tim de Zeeuw, for the allocation of observing time to our program, as well as to the Paranal Observatory team for the successful execution of the observations. This research received the support of PHASE, the high-angular resolution partnership between ONERA, Observatoire de Paris, CNRS, and University Denis Diderot Paris 7. We acknowledge financial support from the Programme National de Physique Stellaire (PNPS) of CNRS/INSU, France. This project has received funding from the European Unions Horizon 2020 research and innovation programme under the Marie Skodowska-Curie Grant agreement No. 665501 with the research Foundation Flanders (FWO) ([PEGASUS][2] Marie Curie fellowship 12U2717N awarded to MM). We used the SIMBAD and VIZIER databases at the CDS, Strasbourg (France)[†], and NASA's Astrophysics Data System Bibliographic Services. This research has made use of Jean-Marie Mariotti Center's **Aspro**[‡] service, and of the **SearchCal** service[§] (co-developed by FIZEAU and LAOG/IPAG). This research made use of IPython (Pérez & Granger 2007) and Astropy[¶], a community-developed core Python package for Astronomy (Astropy Collaboration et al. 2013).

References

Astropy Collaboration, Robitaille, T. P., Tollerud, E. J., et al. 2013, A&A, 558, A33

Aurière, M., López Ariste, A., Mathias, P., et al. 2016, A&A, 591, A119

Baron, F., Monnier, J. D., & Kloppenborg, B. 2010, in Proc. SPIE, Vol. 7734, Optical and Infrared Interferometry II, 77342I

Chiavassa, A., Freytag, B., Masseron, T., & Plez, B. 2011, A&A, 535, A22

Chiavassa, A., Haubois, X., Young, J. S., et al. 2010, A&A, 515, A12

Harper, G. M., Brown, A., Guinan, E. F., et al. 2017, AJ, 154, 11

Haubois, X., Perrin, G., Lacour, S., et al. 2009, A&A, 508, 923

Hestroffer, D. 1997, A&A, 327, 199

Josselin, E. & Plez, B. 2007, A&A, 469, 671

Le Bouquin, J.-B., Berger, J.-P., Lazareff, B., et al. 2011, A&A, 535, A67

Mauron, N. & Josselin, E. 2011, A&A, 526, A156

Montargès, M., Chiavassa, A., Kervella, P., et al. 2017, A&A, 605, A108

Montargès, M., Kervella, P., Perrin, G., et al. 2016, A&A, 588, A130

Montargès, M., Kervella, P., Perrin, G., et al. 2014, A&A, 572, A17

Ohnaka, K., Hofmann, K.-H., Schertl, D., et al. 2013, A&A, 555, A24

Ohnaka, K., Weigelt, G., & Hofmann, K.-H. 2017, Nature, 548, 310

Ohnaka, K., Weigelt, G., Millour, F., et al. 2011, A&A, 529, A163

Pérez, F. & Granger, B. E. 2007, Computing in Science and Engineering, 9, 21

[†]Available at `http://cdsweb.u-strasbg.fr/`
[‡]Available at `http://www.jmmc.fr/aspro`
[§]Available at `http://www.jmmc.fr/searchcal`
[¶]Available at `http://www.astropy.org/`